INSTRUMENTS AND METHODS OF INVESTIGATION

Spectral and spectral-frequency methods of investigating atmosphereless bodies of the Solar system

V V Busarev, V V Prokof'eva-Mikhailovskaya, V V Bochkov

Contents

Abstract. A method of reflectance spectrophotometry of atmosphereless bodies of the Solar system, its specificity, and the means of eliminating basic spectral noise are considered. As a development, joining the method of reflectance spectrophotometry with the frequency analysis of observational data series is proposed. The combined spectral-frequency method allows identification of formations with distinctive spectral features, and estimations of their sizes and distribution on the surface of atmospheresless celestial bodies. As applied to investigations of asteroids 21 Lutetia and 4 Vesta, the spectral-frequency method has given us the possibility of obtaining fundamentally new information about minor planets.

1. Introduction

Lately, the significant increase in the observational capabilities of modern astronomy and, in particular, in planetary astronomy, has led to discoveries of many new objects. For example, the total number of minor planets in the Solar system already approaches 150,000 [1]. However, it should be noted that for almost all new minor planets and satellites only orbital elements are known and estimates of sizes available. Due to a large number of new objects, their physical and chemical – mineralogical characteristics will remain unexplored for a long time. Meanwhile, this information is extremely important for solving several cosmogonical

V V Busarev Sternberg Astronomical Institute, Moscow State University,
Universitetskii prosp. 13, 119992 Moscow, Russian Federation
Tel. (7-495) 939 10 29
E-mail: busarev@sai.msu.ru
V V Prokof'eva-Mikhailovskaya, V V Bochkov Research Institute
'Crimean Astrophysical Observatory',
p/o Nauchnyi, 334413 Crimea, Ukraine
Tel. (380) 65 54 71 124
E-mail: prok@crao.crimea.ua; bochkov@crao.crimea.ua

problems related to the evolution of both minor and major planets of the Solar system. Moreover, solving these problems is relevant not only for our planetary system, but also for the many exoplanetary systems discovered over the last 15 – 20 years [2]. This means that wide use and development of ground-based distant (astrophysical) methods represents a realistic way of rapidly exploring these objects.

Large ground-based telescopes with a mirror diameter of the order of 4 – 10 m would enable the most effective astrophysical studies of minor planets and planetary satellites. However, the actual number of operating telescopes of this class is still small and the observational time on them is strongly limited. So, at the moment it is virtually impossible to count on obtaining a lot of observational data on new planetary objects with these telescopes. The same reasoning applies to observations from space telescopes (Hubble, Spitzer, etc.) and space missions. For these reasons, one should seek the possibility of using for systematic planetary studies intermediate and small-class telescopes (with diameters in the range 0.5 – 3 m) equipped with high-sensitivity detectors. The large number and easy availability of these instruments make the solution of the problem considered realistic in, say, two – three decades. This time could be made shorter if a larger number of specialized observatories for regular planetary observation are constructed. It should be emphasized that the employment of ground-based telescopes to explore the composition and other surface characteristics of solid bodies in the Solar system can be effective only if they lack gas envelopes distorting the reflected solar light.

Successful studies of atmosphereless planets with small telescopes can be carried out using effective methods and highly sensitive detectors. The principal optical methods include, first of all, photometry, spectrometry, and polarimetry of celestial objects. These methods are well elaborated and widely applied in astrophysics, so it is not necessary to describe them in detail. They are also applied to study the structure and characteristics of the surface material of planets.

In this paper, we show how a combination of the two above-mentioned methods and the frequency analysis method (FA) enables us to obtain new information on solid

celestial bodies. These observational methods are based on the property of a cold atmosphereless body to reflect incident solar radiation which can be measured on the detector. Due to a strong roughness of the surface of solid celestial bodies (down to the microlevel where the size of roughnesses is comparable to the optical wavelength), the term 'reflection of a body' implies that the solar light, reflected by the surface of a body, includes both mirror-reflected and scattered components. It should be stressed that the scattered component of interest for us includes the radiation scattered by both the surface (determined by the scattering indicatrix) and the internal volume of the material. It is this latter component of the radiation reflected by a celestial body, which is called the diffusive component, that gives information on the composition of its matter.

If the surface of a body has a spot-like structure or some relief details which have different spectral characteristics or scattering indicatrixes, then the rotation of the body will modulate the radiation flux (spectral or integral) reflected towards the observer. This information is contained in the observational data, and the question arises as to how to extract it correctly. During one complete revolution of a celestial body about its axis of rotation, the observer can register all the changes in the radiation field reflected by the body in the form of brightness variations. The obtained brightness curves (sometimes termed as light curves) give information on details on the surface of the investigated planet in the form of higher harmonics of its rotational frequency. By determining such frequencies across the observed phase interval of the light curve of the planet, one can estimate the characteristic size of inhomogeneities on the corresponding fraction of its surface.

A variant of such FA was applied earlier to the set of photometrical data obtained for the asteroid 1620 Geographer [3]. Its relief sizes were estimated using photometrical observations obtained in 1994 with a time resolution of 0.4 min and 1 min. FA of these data revealed the presence of several periods repeatedly found in three data sets: 5.4, 7.5, and 15 min (the second harmonics of the previous value). In the primary maximum, a long period of around 40 min was present. The amplitudes were found to be small (about $0^m.02$), but were detected quite reliably. The difference in the period values in different maxima of the asteroid light curves suggested different sizes of the details on different sides of the body. For example, the largest and smallest details had a size of $1 - 1.2$ km and $150 - 200$ m, respectively.

The estimates of the surface details of the asteroid 1620 Geographer, obtained by us from FA of photometrical data, were found to be fully consistent with the results of radar studies by Ostro et al. [4]. This enabled us to extend the application of the method under consideration to the area of spectrophotometric and spectral studies of asteroids.

2. On the features of taking planetary reflectance spectra

Let us first consider in more detail the features of the measurement and calculation method for the reflectance spectrum of a planet. This method is somewhat different from the differential spectral measurements well-known in astrophysics. In addition, specialists in the close fields of astrophysics do not always fully understand the physical sense of the term 'the planetary reflectance spectrum' and its relation to the chemical-mineral composition of the matter.

Thus, consider the case (by the way, the most typical for ground-based astronomical observations) where a body is sufficiently small or remote to appear as a point-like source. In addition, we shall assume that the body has no atmosphere. Clearly, these bodies include asteroids, Edgeworth – Kuiper bodies, and atmosphereless satellites of major planets. Then, from measurements in some spectral range of the investigated planet and a standard star, the monochromatic illuminance $E_{\mathrm{p}}(\lambda)$ produced by the planet at the conventional upper boundary of the terrestrial atmosphere can be calculated using the differential photometry method:

$$E_{\mathrm{p}}(\lambda) = E_{\mathrm{ss}}(\lambda) \, \frac{I_{\mathrm{p}}(\lambda)}{I_{\mathrm{ss}}(\lambda)} \, p(\lambda)^{-\delta M} \,, \tag{1}$$

where $E_{\mathrm{ss}}(\lambda)$ (erg cm^{-2} s Å) is the monochromatic illuminance set up by the standard star at the upper boundary of the terrestrial atmosphere, taken, for example, from some publication; $I_{\mathrm{p}}(\lambda)$ and $I_{\mathrm{ss}}(\lambda)$ are the counts of the light intensity from the planet and the standard star, respectively, measured by a spectral detector (CCD or any other) and corrected for the sky background; $\rho(\lambda)$ is the atmospheric spectral transparence function calculated for a given observational night, and $\delta M = M_{\mathrm{p}} - M_{\mathrm{ss}}$ is the air mass difference corresponding to the planet and the standard star at the moment of observations.

On the other hand, according to paper [5], the monochromatic illuminance produced by the planet at the upper boundary of the terrestrial atmosphere (for the normal incidence of the light rays) can be expressed through the monochromatic illuminance $E(\lambda)$ of the investigated planet due to the Sun:

$$E_{\mathrm{p}}(\lambda) = \pi \Gamma_{\lambda} F(\alpha, \lambda) \, E(\lambda) \, \frac{r^2}{\Delta^2} \,, \tag{2}$$

where Γ_{λ} is the geometric albedo accounting for the integral physical – chemical properties of the observed hemisphere of the planet, $F(\alpha, \lambda)$ is the phase function of the planet (for $\alpha = 0$, one has $F(\alpha, \lambda) = 1$), r is the radius of the planet, and Δ is its distance to the Earth. But since the unknown quantity $E(\lambda)$ can be expressed according to the inverse square law through the known (from the literature) solar illuminance $E_0(\lambda)$ at the upper boundary of the terrestrial atmosphere as

$$E(\lambda) = E_0(\lambda) \, \frac{R_0^2}{R^2}$$

(R_0 is the distance from the Earth to the Sun, R is the distance from the planet to the Sun), formula (2) can be recast in the form

$$E_{\mathrm{p}}(\lambda) = \pi \Gamma_{\lambda} F(\alpha, \lambda) \, E_0(\lambda) \, \frac{r^2 R_0^2}{R^2 \Delta^2} \,. \tag{3}$$

Denoting $\rho(\alpha, \lambda) = \pi \Gamma_{\lambda} F(\alpha, \lambda)$, which is called the coefficient (or factor) of the mean spectral brightness of the observed hemisphere of the planet (more precisely, its projection on the observer's plane of the sky), and equating the right sides of expressions (3) and (1) yield the formula for calculation of $\rho(\alpha, \lambda)$ in absolute units:

$$\rho(\alpha, \lambda) = \frac{k E_{\mathrm{ss}}(\lambda) \, I_{\mathrm{p}}(\lambda) \, p(\lambda)^{-\delta M}}{E_0(\lambda) \, I_{\mathrm{ss}}(\lambda)} \,, \tag{4}$$

where $k = \Delta^2 R^2/(r^2 R_0^2)$ is a dimensionless factor. Clearly, $\rho\,(\alpha, \lambda)$ is also dimensionless. If the brightness factor $\rho\,(\alpha, \lambda)$ is considered in some spectral range, its spectral distribution represents the reflectance spectrum. When the phase angle of a planet is close to zero, i.e., $\alpha \approx 0$, the reflectance spectrum constitutes the spectral dependence of the geometrical albedo of the observed hemisphere of the planet.

Equation (4) explains the physical sense of the reflectance spectrum that is obtained by dividing the spectral energy distribution of the planet by the same characteristic of the solar radiation incident on it. The reflectance spectrum of a planet (at least in the near UV, optical, and near IR bands where the proper thermal radiation of the planet is negligible) is the spectral dependence of the diffusive component of the radiation flux that passed through the matter and brings information on its physical-chemical properties.

The present-day practice of planetary spectral studies widely uses the approximate but more simple and convenient method of measuring planetary reflectance spectra, which does not require the detection of the spectral energy distribution of the solar radiation at the moment of observations. Using a solar-like $G0V$ star (for example, from the list in Ref. [6]) as the standard star, one can put $E_{ss}(\lambda) \approx E_0(\lambda)$ into expression (4) and recast it in the form

$$\rho\,(\alpha, \lambda) = \frac{k I_p(\lambda)\, p(\lambda)^{-\delta M}}{I_{ss}(\lambda)} \,. \tag{5}$$

The reflectance spectra of a planet calculated with formula (5) approximate with good accuracy real ones when using the best solar-spectrum analogs. The accuracy of planetary reflectance spectra obtained in this way can be checked by comparing them with similar spectra calculated using different solar analogs or solar spectral data. However, despite obvious advantages, such a simplified method has significant shortcomings due most frequently to a poor quality of the resulting reflectance spectra, i.e., a high noise level. Consider in more detail possible solutions to this problem.

Clearly, a high final signal-to-noise level is required to obtain high-quality planetary reflectance spectra. At the stage of recording of a spectrum, the level of statistical noise can be reduced simply by increasing the exposure time. But the subsequent procedure of dividing spectral data $I_p(\lambda)/I_{ss}(\lambda)$ to obtain the reflectance spectra according to formula (4) or (5) introduces an additional noise component (ANC) into the final result. For example, a low spectral resolution of the detector can be one of the simplest causes of appearing an ANC. In this case, the ANC can result from a poor matching of the spectral scales of the planet and the standard star or the star-analog even if they are correctly calibrated. This error cannot be less than the spectral resolution of the telescope + spectrograph + detector system. If the half-width of some absorption band in the resulting reflectance spectrum turns out to be comparable to the instrumental spectral resolution, its identification is virtually impossible. Increasing the spectral resolution of the detector system enables one to significantly remove this 'source' of the ANC in the planetary reflectance spectra. Let us consider some other causes of appearing the ANC and try to outline ways of removing or constraining it.

The stars themselves taking the part of solar-spectrum analogs serve as the most significant source of the ANC in the planetary reflectance spectra. As is well known from

theoretical and practical astrophysics, in spite of the enormous number and variety of stars there are no ideal solar twins among them because of different values of their physical parameters (the effective temperature, gravity acceleration in the atmosphere, color index, etc.) or chemical composition. Thorough all-sky searches have resulted so far in a list containing only a dozen stars (of 4th–6th magnitudes and spectral classes $G0V - G3V$) which can be considered as good solar-spectrum analogs [7]. A longer list of stars that are considered solar-analog candidates is also being compiled. Relative spectral differences between some stars-analogs and the Sun were analyzed earlier [5]. Paper [5] showed that these differences are most pronounced in the vicinity of the Balmer jump ($0.38 - 0.40$ μm), as well as near the strongest absorption lines (H and K (CaII), H_α, H_β, H_γ, and H_δ). The differences appear not only at wavelengths corresponding to the centers of these lines, but also in the line wings which become more extended with increasing line intensity (in particular, in early-spectral-type stars with increasing T_{eff} or hydrogen content). It also turned out that more shallow spectral inhomogeneities, which appear due to metal lines in spectra of stars-analogs of later spectral classes, can give rise to a noise background in almost the entire visible region of planetary reflectance spectra, when such stars-analogs are used. Thus, when dividing the observed spectrum of a planet (reflecting solar light) to the solar-analog stellar spectrum, the consecutive comparison of the star-analog spectrum and solar spectrum is done. Here, all spectral differences between them can be obtained in the form of a strong ANC which cannot be fully removed. The use of good stars-analogs in this case is the only way to constrain the ANC.

Another significant source of the ANC that is worth considering is the terrestrial atmosphere. As is well known, on the one hand, when solar light passes through the Earth's atmosphere, water vapor, oxygen, carbon dioxide, nitrogen, and ozone give rise to the appearance of intensive telluric lines and bands (see, for example, Ref. [8]). On the other hand, the tiny water droplets and dust in the clouds (even light), as well as atmospheric turbulence cells, cause scattering and fluctuation of light passing through them. Although these scattering phenomena are not spectral-selective, they lead to distortions of the wave front of the radiation flux, which are transformed to its monochromatic components upon spectral decomposition. So, when comparing (dividing) the intensities of radiation fluxes from a planet and a standard star, which passed different optical paths in the terrestrial atmosphere, random fluctuations of their monochromatic components lead to the appearance of the ANC in the resulting planetary reflectance spectrum. Ground-based observations under good sky conditions, as a rule, provide high-quality low-noise spectra of celestial objects. However, for most astronomical observatories (with several exceptions) such atmospheric conditions occur quite rarely and for a limited time period. So looking for new methods for minimizing the ANC in the planetary reflectance spectra obtained from the ground under nonideal sky conditions is a very topical task. Smoothing is quite an effective way of suppressing the ANC in the planetary reflectance spectra. There are several methods, e.g., frequency filtering, running-mean, etc., which improve the quality of the reflectance spectra and help to identify real spectral features. For example, Fig. 1a depicts the reflectance spectrum of the asteroid 21 Lutetia, calculated using the asteroid and solar-analog stellar spectra (HD117176) [March 5, 2006; 1.25-m telescope of the Stern-
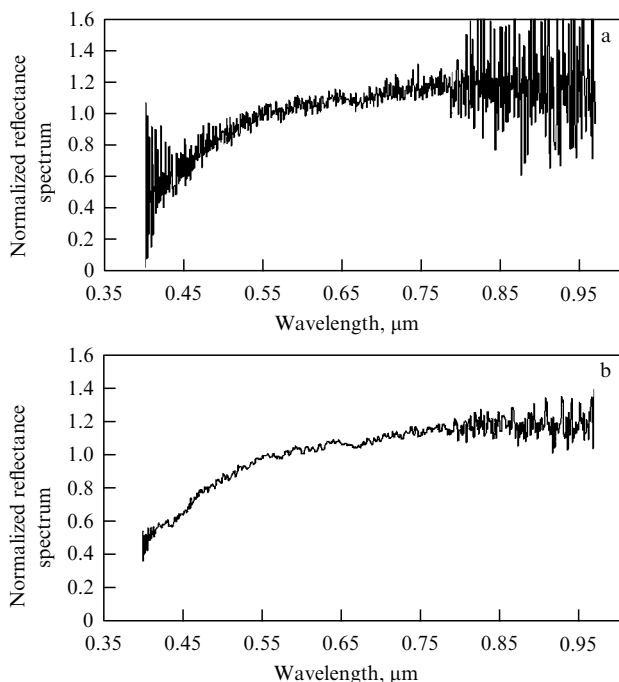
Figure 1. (a) Example of the noisy reflectance spectrum of the asteroid 21 Lutetia. The reflectance spectrum was calculated using the spectra of the asteroid (exposure time 300 s) and the solar analog HD117176 (exposure time 10s) obtained on March 5, 2006 (UT 01^{h}31^m and 03^{h}26^m, respectively) on the 1.25-m telescope of the Crimean Laboratory of SAI with a CCD-spectrograph with a spectral resolution of 0.0009 μm in the 0.40 – 0.96-μm range; the reflectance spectrum was normalized at the wavelength 0.55 μm. (b) The same spectrum after running-mean smoothing over 5 points.

berg Astronomical Institute (SAI) equipped with spectrograph and CCD matrix ST-6] taken under the presence of thin cirrus clouds. Figure 1b shows the same spectrum after smoothing (over 5 points) with the running-mean method. It is seen from Fig. 1b that after the smoothing the asteroid reflectance spectrum (especially near the blue and red edges) retains the noise structure, although with a significantly smaller amplitude.

Below we shall consider special frequency methods that also facilitate identifying and extracting useful information in the reflectance spectra of atmosphereless planets and satellites.

3. Spectral-frequency method

The proposed spectral-frequency method of studies is based on the recording of a sufficiently large number of spectra of a certain atmosphereless solid body and their subsequent FA. As mentioned above, the goal of the method is, first, to discover some structures on the planetary surface and, second, to associate with them the observed variations of the planetary spectral characteristics, which correspond to changes in the physical – chemical parameters of the matter. In the considered FA method, the rotation of a rigid celestial body around its axis is essentially involved. Thus, the repetition of or change in a certain spectral feature (for example, an absorption band) in consecutively taken reflectance spectra of the body studied with a period equal to the rotation period or some fraction of it can serve as proof of its reliability. The measurement of the amplitude of such

periodic variations in 2 – 3 adjacent regions in the reflectance spectrum enables a more complete and reliable description of the spectral shape and its variations and, hence, obtaining more detailed information on the structure inhomogeneities or the composition of the material of this celestial body. Thus, the determination of the frequency (or frequencies) of periodic spectral variations gives the possibility of estimating the sizes and the surface distribution of spectral-contrast spots of the planet's material which has some physical – chemical peculiarities.

Clearly, the necessary condition for the frequency analysis of the spectral data is the measurement of their absolute values. This means that the data obtained at different times and under different conditions (apparatus, atmospheric, and astronomical) must be reduced to a single system with the aid of their calibration, taking outside the terrestrial atmosphere, the reference to stellar standards, and the recalculation to the standard distance of the object from the Earth and the Sun. After such a correction of the original data, in the corresponding spectra of the object studied some characteristic feature can be found (for example, an absorption band or a spectral segment with the particular slope). To describe this feature one, two, or several synthetic photometric bands are calculated. In particular, to characterize an absorption band, it is sufficient to determine its equivalent width; to describe the reflectance spectrum slope in a fixed spectral interval, it is sufficient to calculate the color index, i.e., the ratio of stellar magnitudes of the object in photometric bands chosen at the boundary of this interval.

Modern spectrophotometric equipment provides a good accuracy of measurements (for high signal-to-noise ratios — better than 1%) and high time resolution (up to tenths of a second). During photometric observations in a limited spectral band, radiation fluxes from the solid object studied (a planet) and from neighboring stars are simultaneously detected to control changes in atmospheric extinction (transparency) at night. In the absolute photometry method, the photometric calibration of all observational data is also carried out using an artificial photometric standard [3], and the Earth's atmospheric extinction is determined at each individual night. Such measurements can be made in any spectral band, but the V band providing a sufficiently high signal-to-noise ratio seems to be preferential. FA is performed for the absolute stellar magnitudes of a solid celestial body reduced to a unit distance from the Earth and the Sun and to zero irradiation and observation phase angles. It should be noted that interesting results can also be obtained from FA of the color indices of the object, which can be obtained by dividing its brightnesses in the neighboring spectral bands. This requires simultaneous or quasisimultaneous photometry of the body studied in these spectral bands. Such a color index is free, on the one hand, from the integral changes of the object's brightness related to the observed rotation-induced variations in its shape but, on the other hand, gives information on the distribution of color spots over the body's surface. For example, color spots on different components of a binary object give rise to frequencies in its integral color indices corresponding to the angular rotation velocities of the components, but do not produce the frequency pertaining to their orbital motion.

In order to extract the full information on a celestial object by means of FA of its observational data, the spectroscopy in a wide spectral range (for example, in the entire visible and/or near infrared band) is prefered to broad-band photometry in

one or several spectral bands. Such spectra, as a rule, contain the necessary additional information that can be used for the subsequent choice of narrower photometrical bands. Besides, the synthetic photometric magnitudes of the object in these bands can be evaluated from its known spectral data. These photometric magnitudes can be calculated either in the standard photometric system (for example, the Johnson one), or taking into account the location of some interesting spectral features.

Two approaches to data processing for FA are possible. One is based on the experience of constructing light curves with trial periods and elaborating automatic means of finding the most probable period that minimizes dispersion of data points relative to the mean curve. Different methods of FA rely on different means of estimating the dispersion of points, for example, the Lafler–Kinman method [9] and the Jurkevich method [10]. It should be noted that these methods of FA are applicable to light curves of any form and to series of data with extended breaks. Anyway, to provide a high reliability of finding the true period, a large number of observational points are required. The second approach is based on the Fourier analysis. It is more rigorous mathematically, but its applicability is limited for series with breaks. In 1975, Deeming [11] proposed a method enabling removing frequencies modulated by the series on-off ratio. Recently, the Breger method [12] also based on the Fourier analysis has been widely applied to study brilliance variations in stars and rotating solid bodies. The Breger method is commonly used for preliminary FA of data series. Note that the last two methods can be applicable for objects with sine-like light curves; in the case of light curves with two maxima, they find the second harmonics of the true period.

FA of photometrical data of asteroids obtained at the Crimean Astrophysical Observatory has been performed using a software package enabling frequency searches in light curves of arbitrary shapes. The main program (Period) of data processing was written by M Yu Klepikov and completed by K V Prokof'eva. Here, calculations are simultaneously carried out by three different methods: Lafler–Kinman, Jurkevich, and Deeming [9–11]. The program allows the user to quickly look at the convolution of data with a given period and to find the power of a polynomial to approximate slow changes in the light curve. Subtracting this polynomial from the corresponding photometrical data removes the variations in brilliance with a chosen period, its harmonics, and conjugate periods. In this way, the data whitening is performed, which is required for further searches for hidden periods of smaller amplitudes [13]. If a multiperiodicity is present, the data whitening, as a rule, is carried out in order of decreasing amplitudes of periodic variations.

The complication of the frequency spectrum of astronomical object brilliance in the presence of the series of observations made with extended time breaks is well known in astrophysics as the frequency substitution phenomenon [13]. Frequencies that appear as a result of the interaction of the true frequency of variations in brilliance of the object studied with on-off ones are often called artifacts. The amplitudes of peaks corresponding to these frequencies are comparable to those from the true frequency. In addition, in the frequency spectrum so-called combination or conjugate frequencies that arise when summing the signal with frequencies of the medium the signal passes through are observed [14]. They represent the sum and the difference of the main frequency of the oscillation of the signal from the object studied and the medium frequencies. In FA of astrophysical data, the role of the 'medium' can be played by the on-off ratio of the series analyzed. It carries frequencies determined by the observational conditions — the length of the series or its parts, diurnal, monthly disruptions, and other causes. Note that the use of some *a priori* information, for example, the allowance for two maxima in the light curves of a celestial body, facilitates the estimation of reliability of periods revealed by FA.

Several features are used, as a rule, to find real variations in brilliance of an astronomical object. The detected frequency is considered to be real under the following conditions: in the power spectrum there are harmonics of this frequency and the frequencies of multiple periods, as well as combination frequencies located symmetrically relative to the detected frequency; phase diagrams (convolutions or light curves) constructed with the studied period have no troughs due to the on-off ratio of observations and show the presence of two maxima and two minima of nearly equal amplitudes; phase dependences of the light curves constructed from different series of observations coincide; the peak corresponding to the frequency of a detected period is present in the phase diagrams obtained by different methods, and the periodograms of the model constructed by replacing the observed stellar magnitudes of the object in the series under study by random values, demonstrate no features at the would-be true frequency.

4. Study of the asteroid 21 Lutetia by the spectral-frequency method

The asteroid 21 Lutetia will be one of the most interesting objects to be studied by the Rosetta space mission, which should approach the asteroid in 2010. It belongs to the spectral type M according to the spectral classification by Tolen, and has an albedo of about 0.22 and a diameter of 96 – 100 km [15]. The asteroid moves in an elliptical orbit with eccentricity $e = 0.163$. The orbital inclination is $i = 3.1°$, which allows one to relate it to the plane component of the main asteroid belt (MAB). Its major semiaxis of 2.4369 a.u. points to its location in the inner part of the MAB closer to the middle [16]. The remote distance from the Sun (location in the MAB) and the spectral type suggest the asteroid has passed the stage of magmatic melting, apparently at temperatures of $1000 – 2000\ °C$. This is supported by the quite high albedo of the asteroid. Therefore, one can assume that the surface layer of Lutetia is primarily made of high-temperature minerals (like pyroxenes or olivines) with an admixture of metallic iron [17]. Nevertheless, in opposition to these concepts, the infrared spectrophotometry of Lutetia (near 3 μm) has revealed the presence of connected water or hydroxyl groups in its surface substance [18]. This result may suggest either the erroneous classification of the asteroid or, which is more probable, the action of still unexplored or poorly studied physical and cosmochemical processes by means of which atypical geological materials were delivered to its surface.

It should be stressed that numerous photometrical observations of Lutetia [19–22] revealed irregular variations in brilliance with amplitudes from $0^m.1$ to $0^m.25$, and the most reliable estimate of its rotation period is $8^h.172$ [23]. Spectral observations of Lutetia carried out by Busarev [24] on the 1.25-m and 0.6-m telescopes of the Crimean Laboratory of SAI, and by Bochkov [25] on the 0.5-m meniscus telescope
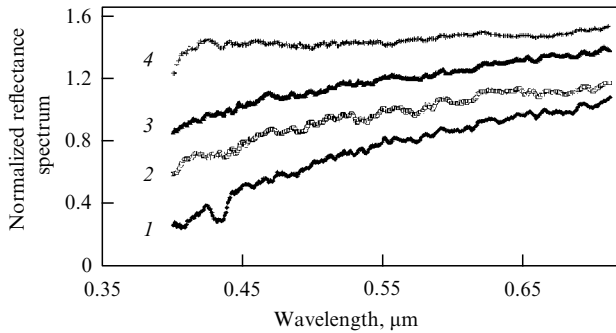
Figure 2. Normalized reflectance spectra of the asteroid 21 Lutetia taken on November 7, 2004 (*UT* 22^{h}21^{m}38^s – 22^{h}40^{m}36^s) with time intervals ~ 10^m at the Crimean Laboratory of the SAI on the 1.25-m telescope with CCD-spectrograph (curves *1*, *3*, and *4* are artificially shifted along the vertical axis for better recognition). Such rapid spectral changes suggest a significant inhomogeneity of the asteroid matter.

(MTM-500) of the Crimean Astrophysical Observatory discovered in the reflectance spectrum of the asteroid a noticeable absorption band centered at 0.430 – 0.440 μm (with a relative deep of up to 8 – 10%), as well as a broad depression at 0.60 – 0.80 μm (Fig. 2). In these observations of the asteroid, the solar analog HD10307 (*G*2V) was used. The same spectral features are found in the reflectance spectrum of Lutetia obtained in March 2006 using another solar analog HD117176 [7] (see Fig. 1). It is seen in Fig. 2 that the reflectance spectrum of the asteroid, obtained in November 2004 under the limitingly small aspect angle of the asteroid (around 43°), varied significantly even over a time interval as short as 10 min. This most likely characterizes the high nonuniformity of the asteroid material structure and composition.

Laboratory studies of the reflectance spectra of the powder of terrestrial hydrosilicates (Fig. 3) [26] showed that the features discovered in the reflectance spectra of Lutetia (the absorption bands near 0.41 – 0.46 and 0.60 – 0.80 μm) are typical for serpentines or a mixture of serpentines with chlorites. This suggested the presence on the surface of Lutetia of an unusual mineralogical combination of high-temperature pyroxenes and olivines (assuming its commonly accepted classification as an *M* type asteroid [15]), as well as of low-temperature serpentized hydrosilicates.

In the period from August 31 to November 20, 2000, about 50 spectra of Lutetia and the same number of spectra of
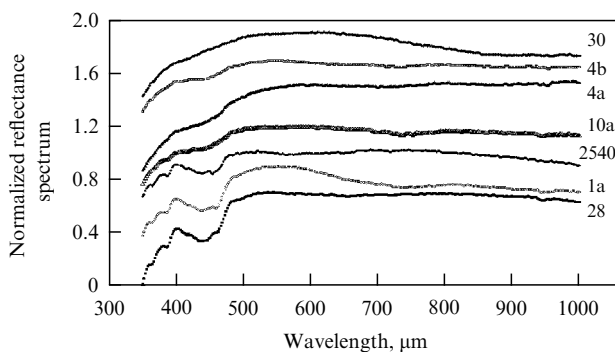

Figure 3. Laboratory normalized reflectance spectra (at the wavelength 550 nm) of terrestrial serpentine powders from different geological occurrences in Russia (1a, 4a, 4b, 10a, 28, 30, and 2540 are the numbers of the probes) (taken from paper [26]).

the solar analog HD10307 and regional standards were obtained at the Crimean Astrophysical Observatory with a resolution of 0.004 and 0.003 μm at the television complex of the MTM-500 telescope. Using these data, the reflectance spectra in the range 0.37 – 0.74 μm were calculated, and equivalent widths of the absorption band centered at 0.44 μm and ascribed to hydrosilicates were obtained. To do so, the continuum line was drawn across normalized reflectance spectra of the asteroid and the equivalent widths of the 0.44-μm absorption band were calculated using the formula

$$W = \sum_{i=1}^{N} \left[1 - r(\lambda_i) \right] \Delta\lambda, \qquad (6)$$

where W is the equivalent width, $\Delta\lambda$ is the spectral step, $r(\lambda_i)$ is the intensity residuals in the spectrum, and N is the number of data points in the band. The random error in the equivalent width determination was found to be 0.00013 μm. Sufficiently rapid equivalent-width variations in this absorption band were observed on the time intervals of about 1 hour. The amplitude of such variations was as high as 0.0012 μm, one order of magnitude higher than the random fluctuations. This allowed us to conclude that the spectral intensity of the luminous flux reflected from the asteroid surface was strongly modulated in the spectral region 0.41 – 0.47 μm, corresponding to the absorption band of serpentines. To study these variations, we performed FA of 40 values of the equivalent width of the absorption band at 0.44 μm and constructed their convolutions (approximation curves) as a function of the rotational phase of the asteroid. For illustration, we present in Fig. 4 one such convolution approximated by a 10-degree polynomial. It has four maxima on the phase interval corresponding to Lutetia's rotation period.

To attain the necessary accuracy of initial data, FA was performed using spectra averaged over 18-min intervals. The Berger program was applied in the frequency range from 5 to 50 cycles per day, and the Deeming program was utilized in the frequency range 40 – 80 cycles per day. For example, we show in Fig. 5 the results of FA in the frequency range from 5 to 50 cycles per day. It is seen that the most significant group of frequencies falls within the interval from 10 to 16 cycles per day. Groups of frequencies with smaller power are found in the ranges 25 – 30 and 38 – 45 cycles per day. To find independent frequencies, the data were whitened for the most pronounced frequencies in order of their decreasing amplitudes by simultaneously applying three FA methods (Lafler – Kinman, Jurkevich and Deeming) [27].

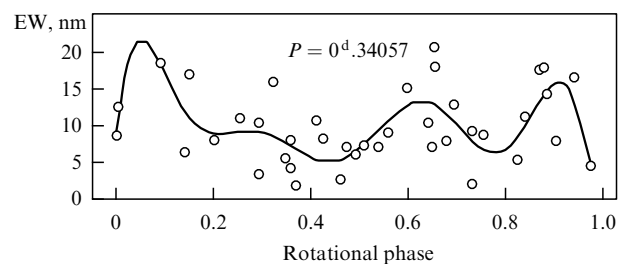

Figure 4. The convolution of the equivalent widths of the hydrosilicate absorption band (EW, nm) centered at 0.44 μm with the rotational period $P = 0^d.34057$ of the asteroid 21 Lutetia. The solid curve is a 10-degree polynomial.
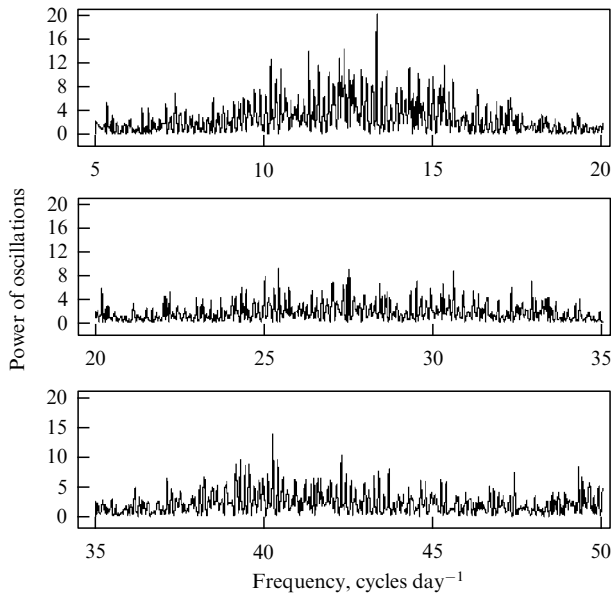
Figure 5. The power spectrum constructed in the frequency range from 5 to 50 cycles per day for variations in the equivalent width of the spectral absorption band of the asteroid 21 Lutetia at 0.44 μm.
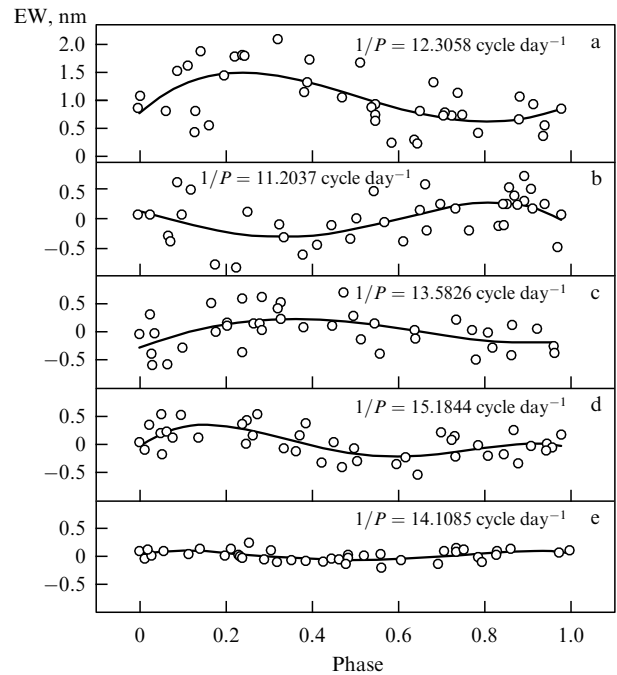

Figure 6. Convolutions of the equivalent widths of the 0.44-μm absorption band in the spectrum of Lutetia (EW, nm) with several periods found. All plots are shown at one scale for both axes. The solid curves represent 4-degree polynomials.

Convolutions of data with some of the periods obtained are illustrated at one scale in Fig. 6. The first four panels show the consecutive data whitening for the periodic variations found. It is seen that the amplitude of variations decreases simultaneously with the dispersion of data points. After the data whitening, the determination accuracy of the equivalent width of the absorption band at 0.44 μm attained 0.0005 μm in extrema and somewhat exceeded the above-mentioned mean accuracy of data (0.00013 μm). In total, 16 significant frequencies were found; their consecutive subtraction allowed us to obtain the data series with a virtually noisy signal. For all corresponding approximating curves (convolutions), the amplitude-to-accuracy ratio (S/N) fell within the range from 7 down to 4, which confirms the reality of their existence.

The values of the detected frequencies are listed in Table 1. The first column shows the frequency in units of the number of cycles per day; the period in days stays in the second column; the frequency amplitude and its determination accuracy (S/N) are in columns three and four, respectively; the fifth column displays the ratio $2P_{rot}/P$ of the rotational period of the asteroid to half the value of each period found; the sixth and seventh columns contain estimates of the size of hydrosilicate spots in degrees and kilometers (for the asteroid diameter 100 km), respectively. The size of each spot was assumed to be determined by about half the distance between the adjacent maxima in the

Table 1. Estimates of sizes of hydrosilicate spots on the surface of Lutetia.

Frequency (inverse days), cycle day^{-1}	Period, day	Amplitude, nm	$\dfrac{S}{N}$	$\dfrac{2P_{rot}}{P}$	Size	
					grad	km
1	2	3	4	5	6	7
6.267	0.1596	0.35	4	4.26	85	73
11.204	0.0893	0.55	5	7.62	47	41
12.306	0.0813	0.90	7	8.37	43	37
13.582	0.0736	0.50	5	9.25	39	34
14.108	0.0709	0.20	4	9.60	37	33
15.184	0.0659	0.50	5	10.33	35	30
30.909	0.0324	0.24	4	21.02	17	15
38.405	0.0260	0.35	5	26.19	14	12
43.40	0.0230	1.2	4	29.60	12.1	10.6
45.54	0.0219	1.5	5	31.10	11.6	10.0
48.08	0.0207	1.0	5	32.44	11.1	9.6
52.93	0.0189	0.9	5	37.84	10.0	8.7
54.97	0.0182	1.0	5	35.84	9.5	8.3
59.07	0.0169	0.5	4	40.06	9.0	7.8
70.09	0.0142	0.4	4	48.64	7.4	6.4
73.42	0.0136	0.6	4	52.36	7.1	6.1

curve of data convolution with the corresponding period. It should be noted that when finding the radiation flux modulation from the rotating asteroid, one first estimates the longitudinal angular size of spots (column 6 in Table 1) and then their linear sizes assuming them to be lying in the equatorial plane of the asteroid (column 7 in Table 1). In reality, they can be located anywhere on its surface. Spots at higher asteroid latitudes can produce the same modulation of the radiation flux as those at the equator, as the longitudinal circumference length depends on the latitude. Assuming high-latitude spots (contributing significantly to the measured luminous flux) to be two times smaller than equatorial ones, the results obtained suggest the presence on Lutetia's surface of hydrosilicate spots with a size from 70 to 3 km. At the same time, it is impossible to exclude the presence of smaller spots on the surface. As noted above, the necessary accuracy of FA was provided by averaging the original spectral data over 18-min intervals, which set the lower limit on the frequencies found in the series of equivalent widths of the absorption band at 0.44 μm.

It is important to stress that Table 1 contains both estimates of hydrosilicate spot sizes on Lutetia's surface and their approximate statistics. Possibly, the statistics are bimodal as one (smaller) maximum of the number of frequencies corresponds to 30–40-km spots, which are apparently related to older craters, and the second (larger) maximum corresponds to 6–10-km spots, which likely resulted from relatively recent impact events. As yet, it is impossible to establish how the craters and spots found on Lutetia's surface are morphologically related, but such a link supposedly exists. So that it is interesting to compare the estimates of sizes and numbers of spots with the size statistics of old and young craters on the Moon, Mars, and Mercury [28]. In paper [28], a total of 11 thousand craters with nonintersecting walls and diameters in excess of 10 km were studied. A statistical analysis revealed that around 70% of the young craters have diameters from 10 to 30 km, 20–25% have diameters from 30 to 60 km, and 7–8% have diameters above 60 km. A similar statistics of the old craters are as follows: approximately 20% of the craters have diameters from 10 to 30 km, about 35% have diameters from 30 to 60 km, and 40–50% have diameters above 60 km. The comparison of these statistics with the obtained estimates of spot sizes on 21 Lutetia possibly suggests that on the asteroid there are more spots associated with young craters, provided that such a correlation of sizes exists.

One of the present authors put forward and elaborated the hypothesis [29–31, 24, 32] that hydrosilicates were delivered on high-temperature type asteroids (*M*, *S*, and *E*) by fragments of silicate-ice bodies from the Jupiter formation zone (BJZ). This hypothesis is based on theoretical results obtained by Safronov and co-authors [33–35], who justified the possibility of the high-velocity ejection (up to several km s^{-1}) of the large BJZ from the Jupiter zone by its embryo at the period it had a mass of 10–20 Earth masses. Perhaps direct high-velocity collisions of a BJZ with some parent bodies of asteroids expelled them forever from the MAB [34]. It is also possible that a significant fraction of matter of more fragile and, compared to the asteroids, composition-inhomogeneous BJZ has been retained after such collisions in the MAB in the form of lower-velocity smaller fragments and dust. Such small bodies could have fallen for a long time to the remaining asteroids and nearby planets and could even form on their surface a layer with an atypical composition [32].

Here, it is important to emphasize that, unlike the parent bodies of asteroids, which have predominantly a silicate composition [16, 17], the material of the BJZ, which was originally enriched with volatiles (including H$_2$O), at a period under discussion could already have been made of ready hydrosilicates. Due to the possible radionuclide heating of the BJZ depths by short-lived isotopes (mainly ^{26}Al) during the first several million years of their life, a liquid water ocean probably existed in their interiors where hydrosilicates could have been formed from ordinary silicates (olivines, pyroxenes, etc.) [36].

Thus, a very plausible 'scenario' for the delivering to asteroids of the material of the BJZ that remained in the MAB after the primordial impact events consists in its gradual precipitation in the form of small particles and dust under relatively small velocities, which provided for the conservation of water compounds involved [32]. Such secondary processes and later impacts could result in a spot-like distribution of hydrosilicates over the surface of those asteroids in which such compounds could not form because of the magmatic origin of their parent bodies (at temperatures up to 1000–2000 °C). These include asteroids of *E*-, *S*-, and *M*-types which, as follows from distant studies (including radar ones), are predominantly made of high-temperature silicates like pyroxenes and olivines with a possible admixture of nickel iron [17]. This assumption gains observational support from studies of the integral and spectral modulation of the radiation flux reflected from 21 Lutetia's surface. Thus, the results of the authors confirm the hypothesis for the delivery of hydrosilicates to the surface of this asteroid during low-velocity collisions with small hydrotated bodies or by the gravitational capture of a hydrosilicate-bearing dust. It should be noted that there are two possible interpretations of the nature of such spots on Lutetia's surface: either they are craters formed during low-velocity collisions of the asteroid with small hydrotated bodies and are filled with the material of such 'impactors' or, in contrast, they represent areas between younger craters covered by hydrosilicate dust which hides the matter with another (primeval for the asteroid) composition.

Here, we presented only part of the results of spectral-frequency studies of the asteroid Lutetia. We do not discuss here other published results [37, 38] of its spectral, spectro-photometrical, and photometrical (*BVR*) studies that enabled its binarity to be established.

For comparison, it is worth considering here some new results of spectral-frequency studies of another asteroid — 4 Vesta, which were obtained at the Crimean Astrophysical Observatory.

5. Color spots on the surface of the asteroid 4 Vesta

The surfaces of asteroids are known to be very inhomogeneous in optical characteristics which are determined by the structure and composition of their matter. As early as 1983, L A Akimov et al. [39] noted that asteroid surfaces are much more nonuniform than was thought before. The effect of inhomogeneities on the solar radiation flux scattered by the visible hemisphere of any asteroid is determined by the amount of the reflected light and can vary by 10–15% on different parts of the surface. The law suggested by Akimov and co-workers well describes light scattering by highly rough surfaces. The Moon, asteroids, and most other atmosphere-

less bodies in the Solar system, which were subjected to intensive impact action, have such surfaces [40].

The above-described spectral-frequency method of studying atmosphereless bodies was also applied to estimating the size and clarifying the nature of color spots found on the asteroid Vesta. Interest in observations of this asteroid has significantly increased after its inclusion in the target list of the space mission Dawn. The launch of the Dawn mission has been moved from 2006 to 2007 and the spacecraft is scheduled to approach and orbit Vesta in 2011.

Vesta is the third by size and the brightest of the asteroids. Its form is almost spherical, which causes only one maximum and one minimum to appear in its light curve [41]. The asteroid's diameter is estimated to be 555 km [42], however there are other estimates [43–46]. The high brightness of the asteroid is due not only to the large size but also to a high surface albedo of 0.25 [47, 39]. The geometrical albedo of the visible hemisphere changes by about 7% during one rotational period [48]. The light curve shows a variable amplitude from $0^m.15$ to $0^m.085$ [49, 50] that is caused by the aspect change during the orbital motion of the asteroid. The rotation period equals 5.342 h [51, 41]. The surface of the asteroid is inhomogeneous, as is evidenced by the spectral and brightness variations. Color index variations of Vesta as a function of the rotational phase were found from UBV-photometry [52]. Speckle-interferometric observations revealed the presence of about 100-km spots on the asteroid's disk [45]. Asteroid observations carried out from the Hubble Space Telescope established the presence of spots in sizes down to 80 km on its surface. In addition, a huge crater 460 km in diameter was discovered near the south pole [46]. Apparently, a destructive impact with the asteroid occurred, producing a family of Vesta, including up to 200 members [53]. There is evidence of a genetic relation of basaltic achondrite meteorites with Vesta [54]. It is assumed that the asteroid passed the phases of heating, melting, and matter differentiation, which led to the formation of a metallic core and basaltic crust, similar to the lunar maria [46]. It is thought that the high-temperature phase should have removed water compounds from the asteroid. However, recent observations carried out by Japanese astronomers in Hawaii found signatures of water compounds on its surface [55]. Like the case with the asteroid 21 Lutetia, such water compounds could have been brought to Vesta during its collisions with more primitive bodies.

Spectrophotometric observations of the asteroid Vesta were carried out on 2–4 and 7 February 2002 at the Crimean Astrophysical Observatory at the television complex of the MTM-500 telescope. Spectra were taken by a slitless afocal spectrograph with transparent diffraction grating (200 lines per mm). The exposure time was 30 s. The region standard BS1201 was recorded every 30–55 min. A total of 690 spectra of the asteroid were measured. In addition, averaging over three consecutive observations was performed to increase the accuracy.

Synthetic stellar magnitudes of the asteroid were calculated in the spectral bands shown in Fig. 7. The R-band was narrowed due to the low sensitivity of the radiation detector in the red band. The effective wavelengths of the bands were close to those of the standard B-, V-, and R-bands of the Johnson–Morgan photometric system. The synthetic stellar magnitudes obtained were used to calculate the asteroid colors B-V and V-R with an accuracy of about $0^m.005$. Frequency analysis of the color indices confirmed the known rotation period $5^h.342$ ($0^d.2225$) of the asteroid.
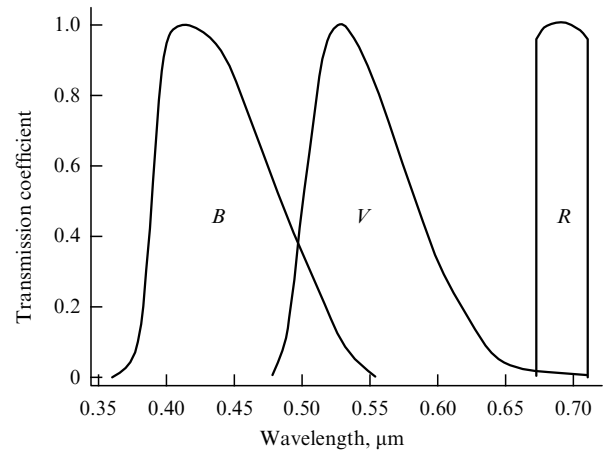

Figure 7. Normalized spectral transmission curves used for calculations of stellar magnitudes of the asteroid Vesta in the spectral bands B, V, R on the basis of extra-atmospheric spectra obtained in observations.

Convolutions of the color indices B-V and V-R with the asteroid rotation period revealed their variations with the amplitude $0^m.04$. Then the data were whitened for the asteroid rotational frequency and sequential searches for higher frequencies were carried out. Oscillations were detected in the total range of 4–90 cycles per day. It should be noted that the search for each new frequency was preceded by whitening the data for the previously found frequency. The Deeming program [12] based on the Fourier transformation was applied. The data convolutions were constructed for each of the frequency found. The amplitudes of the oscillations found were discovered to fall within the limits from $0^m.03$ to $0^m.005$, with the latter value having been obtained only once. As the dispersion of data points gradually decreased in the course of the data whitening, the amplitudes of all convolutions corresponding to the frequencies found exceeded their determination errors by 6–3 times. This suggests a sufficient significance of all these frequencies. The results obtained for color indices B-V and V-R are presented in Fig. 8.

The frequencies found were used to estimate the size of color spots on the asteroid's surface by the method described above in the analysis of variations in the equivalent widths of the absorption band at 0.44 μm in the reflectance spectrum of the asteroid 21 Lutetia. Therefore, here we give only final results (see Tables 2 and 3). As in the case of Lutetia, the size estimation of spots on Vesta was done assuming their equatorial location. Frequencies determined from the analy-

Table 2. Sizes of spots on the surface of the asteroid Vesta, as derived from the B-V color index.

Frequency, cycle day^{-1}	5.9	15	20	26	30	34	51	58	80
Size, km	650	250	180	150	124	112	72	65	46

Table 3. Sizes of spots on the surface of the asteroid Vesta, as derived from the V-R color index.

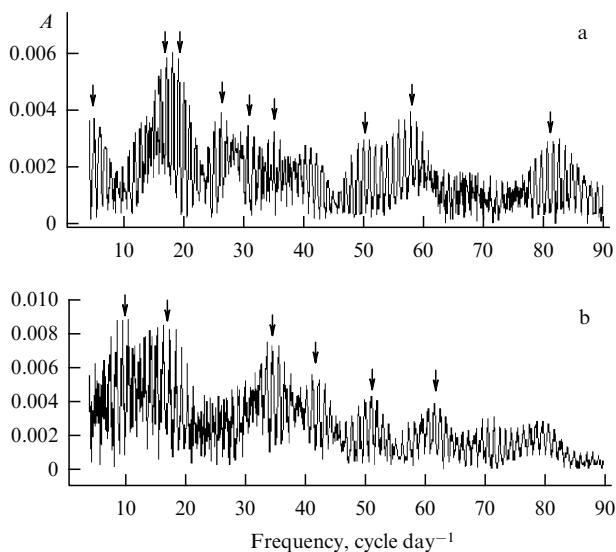| Frequency, cycle day^{-1}	10.6	17.4	35.6	42.4	51.2	61.2
Size, km	360	220	115	90	70	60

Figure 8. The frequency amplitude spectrum of color indices *B-V* (a) and *V-R* (b) of the asteroid Vesta, whitened for the rotational period of the asteroid. Frequencies from 4 to 90 cycles day^{-1} are shown. Arrows mark the location of the frequencies found.

sis of the color index variations in Vesta are shown by arrows in Fig. 8. They are also shown in Tables 2 and 3 for color indices *B-V* and *V-R*.

Nine independent frequencies were discovered in variations of the color index *B-V* of Vesta (see Fig. 8a and Table 2). They were used to estimate the sizes of the corresponding color spots. The largest and smallest equator-reduced sizes were 650 km and 46 km, respectively. The estimated sizes of spots decrease with latitude in the case of their location closer to the pole. If the size of the biggest crater (460 km in diameter) discovered at the south pole of Vesta is increased by a factor of 1.4 (which corresponds to an approximate correction coefficient of the linear scale for a spherical segment), we shall arrive at the size found for the largest spot, 650 km. This suggests the presence of a relation between these formations. Because the largest spot did not manifest itself in the red color range (there are no maxima at frequencies of 5 – 6 cycles per day in Fig. 8b), a bluish color of the biggest crater on Vesta may also be suggested, which probably implies a relatively young age of this impact formation. Spectral studies of lunar ground probes brought to Earth showed that a reddish color is typical for matured material that has been subjected to long-term processing by cosmogenic factors like micrometeorite and solar charged particle (solar wind) bombardment [56]. The conclusion was then made that the reddish color of the matured silicate material, or increasing its reflective properties with wavelength in the visual range, results from its saturation by remelted or vitrified particles enriched with metal ions.

An analysis of the *V-R* color index demonstrated the presence of six most pronounced frequencies. They are shown by arrows in Fig. 8b and are central in frequency groups. The mean frequencies and the corresponding mean sizes of asteroid's equatorial spots are listed in Table 3.

Comparison of color spot sizes derived from color indices *B-V* and *V-R* (Tables 2 and 3) reveals the presence of nearly equal-sized details: 250 and 220 km, 115 and 112 km, 72 and 70 km, 65 and 60 km, respectively. At the same time, there are features (with sizes of 650, 150, 124, and 46 km) which are

visible only in the short-wavelength part of the spectrum. The entire range of Vesta spot sizes at short wavelengths is generally two times as broad as at long wavelengths. This also likely suggests a lower age of blue formations on the asteroid compared to red ones. As is well known, continuous treatment of the surface of atmosphereless bodies in the Solar system by meteorite and micrometeorite bombardment destroys older structures.

Thus, the frequency analysis of the solar radiation scattered by the visible hemisphere of Vesta revealed a 3 – 2% modulation depth for the reflected flux due to the presence of color spots on its surface. Estimated sizes of these spots fall within the range from 46 to 650 km, with noticeable differences at short and long wavelengths. Note that the size estimates of the surface details of the asteroid 4 Vesta are consistent with results of speckle-interferometric observations and observations carried out by the Hubble Space Telescope.

6. Conclusions

The development of observational methods for astronomical objects, including atmosphereless bodies of the Solar system, as well as methods for spectral data analysis, enables us to elaborate new spectral-frequency methods for their study.

The reflection of solar radiation directly by the surface of solid atmosphereless bodies gives the possibility of directly probing them by optical methods. It is important to stress that solar radiation scattered by such a body gives information not only on the large-scale structure and roughness of its surface, but also on the composition of the surface material. The proper rotation of cosmic solid bodies modulates the reflected radiation (integral or monochromatic), and the modulation frequencies contain information about the amplitude and character of nonuniformities of the bodies. Although being rather small (sometimes a few percent), this modulation can be reliably registered by modern detectors.

The experience in studying the asteroids 21 Lutetia and 4 Vesta by the spectral-frequency method demonstrates its high efficiency for discovering some surface-structure features or composition peculiarities of the asteroids and estimating observed surface distributions of relevant formations. This method allowed us to obtain principally new information about these asteroids. In particular, the discovery of hydrosilicates on Lutetia was made, and their surface distribution, sizes, and statistics were investigated, though the latter in the first approximation. The hydrosilicate spots on Lutetia's surface were found to have, generally, small sizes from 6 to 10 km, suggesting their relatively recent origin. It should be stressed that the minimum size of these formations is limited by the time resolution (more precisely, time averaging) of our observations. Thus, these results lend further support to the hypothesis for the origin of hydrosilicates on the surface of Lutetia and other magmatic type asteroids as being due to their delivery by hydrosilicate-bearing small bodies and/or dust.

Broad-band (*B*, *V*, and *R*) spectral studies of one of the largest asteroids, 4 Vesta, carried out by the authors, enabled us to discover and to estimate the sizes of color spots on the asteroid's surface in the blue and red spectral bands. In particular, the biggest spot in the blue band corresponds to the size of the largest crater resided in the southern hemisphere of the asteroid. At the same time, this formation is not seen in the red band, which may suggest its relatively young age.

It should be noted that new methods proposed by the authors can also be applicable to studies of all atmosphereless bodies, including artificial satellites of the Earth. Presently, their number is quite large, so the elaboration of methods is needed that would allow their precise identification and help to solve inverse problems related, for example, to the determination of their form and construction details.

The authors acknowledge A N Abramenko, the leading engineer of the Research Institute 'Crimean Astrophysical Observatory', for maintaining the television complex MTM-500 at high scientific and technical levels.

References

1. Discovery Circumstances: Numbered Minor Planets, http://www.cfa.harvard.edu/iau/lists/NumberedMPs.html
2. The Extrasolar Planets Encyclopaedia, http://exoplanet.eu/catalog.php
3. Karachkina L G, Prokof'eva V V, Tarashchuk V P *Astron. Vestn.* **32** 327 (1998) [*Solar Syst. Res.* **32** 287 (1998)]
4. Ostro S J et al. *Icarus* **121** 46 (1996)
5. Busarev V V *Astron. Vestn.* **33** 140 (1999) [*Solar Syst. Res.* **33** 120 (1999)]
6. Hardorp J *Astron. Astrophys.* **91** 221 (1980)
7. Cayrel de Strobel G *Astron. Astrophys. Rev.* **7** 243 (1996)
8. Kurt V G, in *Fizika Kosmosa*: *Malen'kaya Entsiklopediya* (Physics of Cosmos: Small Encyclopedia) 2nd ed. (Ed. R A Sunyaev) (Moscow: Sovetskaya Entsiklopediya, 1986) p. 505
9. Lafler J, Kinman T D *Astrophys. J. Suppl.* **11** 216 (1965)
10. Jurkevich I *Astrophys. Space Sci.* **13** 154 (1971)
11. Deeming T J *Astrophys. Space Sci.* **36** 137 (1975)
12. Breger M *Commun. Astroseismol.* (111) 1 (1990)
13. Terebizh V Yu *Analiz Vremennykh Ryadov v Astrofizike* (Analysis of Time Series in Astrophysics) (Moscow: Nauka, 1992)
14. Gorelik G S *Kolebaniya i Volny*: Vvedenie v Akustiku, Radiofiziku i Optiku (Oscillations and Waves: Introduction to Acoustics, Radio Physics and Optics) 2nd ed. (Moscow: Fizmatgiz, 1959) p. 409
15. Tedesko E F, in *Asteroids II* (Eds R P Binzel, T Gehrels, M S Matthews) (Tucson: Univ. of Arizona Press, 1989) p. 1090
16. Bell J F et al., in *Asteroids II* (Eds R P Binzel, T Gehrels, M S Matthews) (Tucson: Univ. of Arizona Press, 1989) p. 921
17. Gaffey M J, Bell J F, Cruikshank D P, in *Asteroids II* (Eds R P Binzel, T Gehrels, M S Matthews) (Tucson: Univ. of Arizona Press, 1989) p. 98
18. Rivkin A S et al. *Icarus* **117** 90 (1995)
19. Lupishko D F et al. *Kinemat. Fiz. Nebes. Tel* **3** (5) 36 (1987)
20. Lupishko D F, Velichko F P *Kinemat. Fiz. Nebes. Tel* **3** (1) 57 (1987)
21. Michalowski T *Icarus* **106** 563 (1993)
22. Dotto E et al. *Astron. Astrophys. Suppl. Ser.* **95** 195 (1992)
23. Michalowski T *Icarus* **123** 456 (1996)
24. Busarev V V *Astron. Vestn.* **36** 39 (2002) [*Solar Syst. Res.* **36** 35 (2002)]
25. Bochkov V, Busarev V, Prokof'eva V V *Astron. Astrophys.Trans.* **22** 621 (2003)
26. Busarev V V et al., in *40th Vernadsky Inst. — Brown Univ. Microsymp. on Comparative Planetology, October 11–13, 2004, Moscow, Russia*, Abstract No. 15
27. Prokof'eva V V, Tarashchuk V P, Gor'kavyĭ N N *Usp. Fiz. Nauk* **165** 661 (1995) [*Phys. Usp.* **38** 623 (1995)]
28. Skobeleva T P *Astron. Vestn.* **21** 221 (1987)
29. Busarev V V *Icarus* **131** 32 (1998)
30. Busarev V V, in *31st Annual Lunar and Planetary Science Conf., March 13–17, 2000, Houston, TX, USA* (LPI Contribution No. 1000), Abstract No. 1428
31. Busarev V V, in *32nd Annual Lunar and Planetary Science Conf., March 12–16, 2001, Houston, TX, USA* (LPI Contribution No. 1080), Abstract No. 1927
32. Busarev V V, in *35th Lunar and Planetary Science Conf., March 15–19, 2004, League City, TX, USA* (LPI Contribution No. 1197), Abstract No. 1026
33. Safronov V S, in *Asteroids* (Ed. T Gehrels) (Tucson: Univ. of Arizona Press, 1979) p. 975
34. Safronov V S, Ziglina I N *Astron. Vestn.* **25** 190 (1991)
35. Ruskol E L, Safronov V S *Astron. Vestn.* **32** 291 (1998) [*Solar Syst. Res.* **32** 255 (1998)]
36. Busarev V V, Dorofeeva V A, Makalkin A B *Earth, Moon, Planets* **92** 345 (2003)
37. Prokof'eva V V, Bochkov V V, Busarev V V *Astron. Vestn.* **40** 512 (2006) [*Solar Syst. Res.* **40** 468 (2006)]
38. Busarev V V, Prokof'eva V V, Bochkov V V, in *38th Lunar and Planetary Science Conf., March 12–16, 2007, League City, TX, USA* (LPI Contribution No. 1338), Abstract No. 1016
39. Akimov L A, Lupishko D F, Bel'skaya I N *Astron. Zh.* **60** 999 (1983) [*Sov. Astron.* **27** 577 (1983)]
40. Akimov L A, Lupishko D F, Shevchenko *Astron. Vestn.* **26** (4) 62 (1992)
41. Aksenov A N et al. *Pis'ma Astron. Zh.* **13** 616 (1987) [*Sov. Astron. Lett.* **13** 257 (1987)]
42. Degewij J, Tedesco E F, Zellner B *Icarus* **40** 364 (1979)
43. Worden S P et al. *Icarus* **32** 450 (1977)
44. Drummond J, Eckart A, Hege E K *Icarus* **73** 1 (1988)
45. Tsvetkova V S et al. *Icarus* **92** 342 (1991)
46. Thomas P C et al. *Science* **277** 1492 (1997)
47. Gehrels T *Astron. J.* **72** 929 (1967)
48. Cellino A et al. *Icarus* **70** 546 (1987)
49. Blanko C, Catalano S *Icarus* **40** 359 (1979)
50. Melillo F J *Minor Planet Bull.* **22** 19 (1995)
51. Taylor R C, Tapia S, Tedesco E F *Icarus* **62** 298 (1985)
52. Reynoldson G et al. *Minor Planet Bull.* **20** 11 (1993)
53. Burbune T H et al., in *Asteroids, Comets, Meteors*: *Cornell Univ., USA, July 26–30, 1999*, Abstract, p. 52
54. Binzel R P, Xu S *Science* **260** 186 (1993)
55. Hasegawa S et al. *Geophys. Res. Lett.* **30** (21) PLA 2 (2003)
56. Charette M P et al. *J. Geophys. Res.* **79** 1605 (1974)